High-power widely tunable thulium fiber lasers

Timothy S. McComb,[1,2] R. Andrew Sims,[1] Christina C. C. Willis,[1] Pankaj Kadwani,[1] Vikas Sudesh,[1,3] Lawrence Shah,[1,*] and Martin Richardson[1]

[1]Townes Laser Institute, CREOL, University of Central Florida, 4000 Central Florida Boulevard, Orlando, Florida 32816, USA

[2]Currently with Northrop Grumman Aerospace Systems, One Space Park, Redondo Beach, California 90278, USA

[3]Currently with Quantum Technology, Inc., 108 Commerce Street, Lake Mary, Florida 32746, USA

*Corresponding author: lshah@creol.ucf.edu

Received 12 August 2010; revised 4 October 2010; accepted 9 October 2010; posted 11 October 2010 (Doc. ID 132948); published 3 November 2010

Applications requiring long-range atmospheric propagation are driving the development of high-power thulium fiber lasers. We report on the performance of two different laser configurations for high-power tunable thulium fiber lasers: one is a single oscillator utilizing a volume Bragg grating for wavelength stabilization; the other is a master oscillator power amplifier system with the oscillator stabilized and made tunable by a diffraction grating. Each configuration provides >150 W of average power, >50% slope efficiency, narrow output linewidth, and >100 nm tunability in the wavelength range around 2 μm. © 2010 Optical Society of America

OCIS codes: 140.3510, 140.3600, 050.7330.

1. Introduction

Thulium lasers are of interest for numerous and diverse applications, most prominently for applications requiring long-range propagation through the atmosphere, such as directed energy, infrared optical countermeasures, and remote sensing. Thulium-doped silica offers the potential to efficiently lase from ~1.8 to 2.1 μm [1], a spectral region within the eye-safe regime including windows of high transparency and strong absorption in air. As such, there are two primary categories of application; those that seek to minimize atmospheric absorption, such as directed energy [2] and free-space optical communication [3], or those such as lidar that rely upon narrow molecular vibration absorption resonances to sense atmospheric constituents such as water vapor and CO_2 [4–6]. However, tunable high average power sources have only recently become available in this wavelength range, and little experimental data on long-range atmospheric propagation are available.

Thulium-doped silica fiber lasers take advantage of the well-known cross relaxation process that allows an ~80% theoretical slope efficiency when pumping with 792 nm diodes [7,8], and >70% slope efficiencies have been realized experimentally [9]. The availability of high-power commercial diodes and the inherent thermal management advantages of the fiber laser architecture have enabled the rapid development of high-power thulium fiber lasers [10,11]. However, many promising applications for Tm:fiber lasers require spectral control in terms of both tunability and linewidth. Fiber Bragg gratings (FBGs) are often used for spectral selection in fiber lasers [12], but there are difficulties achieving sub-nm spectral widths particularly in combination with large mode area (LMA) fibers [13], and the tuning range of FBGs is limited by the mechanical strength of the fiber typically to a few tens of nanometers [14]. Other elements for wavelength stabilization and narrowing include volume Bragg gratings (VBGs) [15,16] and guided mode resonance filters [17,18].

0003-6935/10/326236-07$15.00/0

For broad tunability, most efforts to date have relied upon conventional diffraction gratings [19,20]. Recently, high-power narrow linewidth oscillators have been demonstrated [16,21]; however, master oscillator power amplifier (MOPA) architectures generally offer higher performance and greater performance flexibility [22,23], particularly where broad tunability is concerned [9,20].

This paper reports on two high average power tunable thulium fiber laser configurations producing more than 150 W average power with narrow output linewidth, nearly diffraction-limited beam quality, and over 100 nm tunability around 2 μm. The first is a conventional MOPA configuration in which the oscillator is optimized for wide tunability and narrow linewidth, while the power amplifier (PA) is optimized for high power and efficiency. The PA is based upon a 25 μm core, 400 μm cladding thulium-doped silica LMA fiber, and it delivers more than 200 W average power from 1927 to 2097 nm with sub –200 pm linewidth, and $<$1.2 M^2. The PA is modified into a high-power oscillator for the second configuration using a high-power VBG, offering a significantly simplified setup producing $>$150 W at 2052 nm, $<$1.5 nm linewidth, and $>$100 nm laser tunability at 48 W average power.

2. Laser Setup

A. Moderate Power Level Master Oscillator

The MOPA (Fig. 1) is composed of a moderate power level master oscillator (MO) providing a broad tuning range and $<$200 pm linewidth, and a single pass PA efficiently generates high power with nearly diffraction-limited beam quality.

The MO is based on a polarization maintaining (PM) single-mode thulium doped fiber with 10 μm, 0.16 NA core and 0.46 NA, 130 μm cladding (Nufern Inc.). The active fiber is wrapped around an 8 cm diameter mandrel cooled to ~14 °C, and passive fiber is spliced to both ends of the active fiber for thermal management. The output fiber facet is perpendicularly cleaved to form an output coupler, and the output fiber includes a cladding mode stripper to insure that the output beam is completely confined in the core. The other end of the active fiber is spliced to

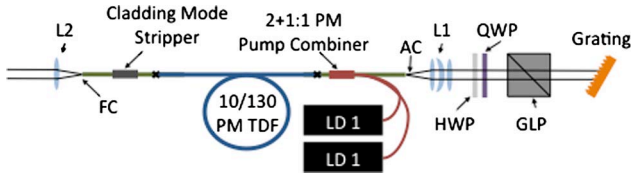

Fig. 1. (Color online) Master oscillator schematic.

a 2 + 1:1 pump combiner (Avensys/ITF Labs) with a matched PM 10/130 pass-through fiber and 100/125 μm core/cladding pump input fiber, limited to 25 W per input. The pump diodes are two 40 W, 100 μm fiber-coupled 790 nm diodes (Dilas Diodenlaser GmbH). The free end of the pass-through fiber is cleaved at ~8° to angle, and its output is collimated to an ~8 mm diameter beam by a 26 mm focal length Infrasil aplanatic triplet lens. A quarter- and half-wave plate, a polarizing beam splitter cube, and a diffraction grating complete the cavity. We use the quarter-wave plate to compensate for variations in retardation with wavelength that occur with just a half-wave plate alone (designed for 2050 nm) over our $>$170 nm tuning range, allowing more stable operation of the MO. We chose a conventional diffraction grating for wavelength control, as it inexpensively provides a large continuous tuning range. The wave plates and beam cube in combination with the PM fiber provide a high polarization extinction ratio (PER) of ~20 dB. The diffraction grating consists of a gold coating on a copper substrate with a 600 line/mm ruling, blazed for 1.9 μm. It is mounted on a rotation stage for tunability and is thermoelectrically cooled for stable laser operation.

An 11 mm focal length single-element TAC-4 glass aspheric lens collimates the laser output and sends it through an additional quarter- and half-wave plate pair for polarization adjustment before transmission through a free-space optical isolator designed for 2050 nm (OFR, a division of Thorlabs, Inc.). The seed from the MO is coupled into the PA by a 26 mm focal length Infrasil aplanatic triplet lens, which matches the mode fields between the single-mode MO and the LMA amplifier.

The PA (Fig. 2) is based on a 5 m long section of ~4 wt.% thulium-doped LMA fiber with a 25 μm diameter 0.09 NA core and a 400 μm diameter 0.46 NA

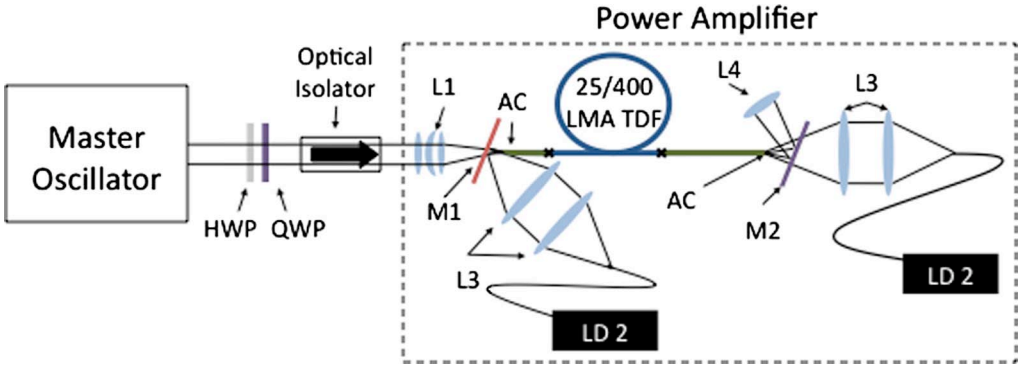

Fig. 2. (Color online) Power amplifier schematic.

octagonal cladding (Nufern, Inc.). The active fiber is wrapped around an 11 cm diameter mandrel that is cooled to ~14 °C to promote efficient two-for-one cross relaxation [8]. Both ends of the active fiber are spliced to ~1.5 m long sections of passive fiber with matched core and cladding. The splices and the fiber ends are held straight in cooled V grooves to facilitate high-power bidirectional free-space end pumping by two 300 W, 793 nm diodes with 400 μm diameter 0.22 NA delivery fiber (Lissotschenko Mikrooptik GmbH). The pump light is 1:1 imaged into both ends of the 25/400 double-clad fiber via a pair of 100 mm focal length 0.26 NA achromatic lenses, and launched either by transmission through or reflection from an appropriate dichroic mirror (Fig. 2). The total pump coupling efficiency is ~75%. The optomechanical and thermal management design of the system is such that continuous or intermittent operation at full power is possible with minimal adjustment over several hours. The input fiber facet is angle cleaved to ~8°, and the output facet is cleaved at ~10° to frustrate parasitic lasing. The output facet is cleaved at a larger angle so that any amplified spontaneous emission (ASE) or parasitic lasing exists with the main output rather then feeding back to the MO. The PA output is directed off of a dichroic mirror and is collimated with a 50 mm focal length Infrasil aplanatic triplet lens.

B. High-Power Oscillator

The two high-power oscillator configurations (Fig. 3) are modified versions of the PA, using the same fiber, pump diodes, and optomechanical components. In this oscillator configuration, the output fiber end is perpendicularly cleaved so that Fresnel reflection from the fiber facet serves as the output coupler, while the intracavity fiber end is cleaved to ~8° to mitigate parasitic lasing.

The intracavity lens (L1) is an antireflection (AR)-coated 26 mm focal length Infrasil aplanatic triplet that collimates the beam to an ~3 mm diameter. For fixed wavelength operation, a VBG is inserted at normal incidence, providing high reflectivity in the spectral band, as shown in Fig. 4A. For comparison, a standard high-reflection (HR) mirror is used for intracavity feedback to characterize the performance of the system with no wavelength selective optics in the cavity. For tunable operation, the VBG is mounted on a rotation stage to vary the angle of incidence to the grating and thereby change the Bragg condition, as shown in Fig. 4B, and an additional HR mirror reflects the beam back to the VBG, as shown in Fig. 3B.

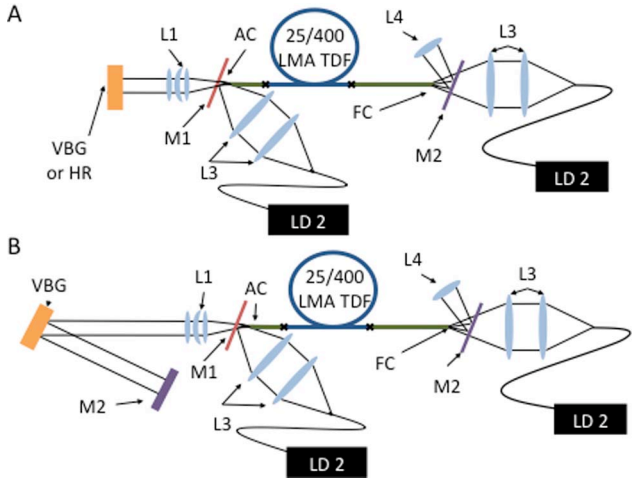

Fig. 3. (Color online) High-power oscillator schematics.

3. Laser Performance

A. MOPA

Figure 5A shows the MO tuning range with continuous tunability from 1907 to 2098 nm with ~8 W output power (sufficient to seed the PA). The short wavelength end of the tuning range is limited by reabsorption associated with the three-level nature of the thulium ion. At longer wavelengths, performance is limited by a lower thulium emission cross section and background absorption losses in the silica glass host material. The long wavelength performance could be improved to up to 2180 nm with the addition

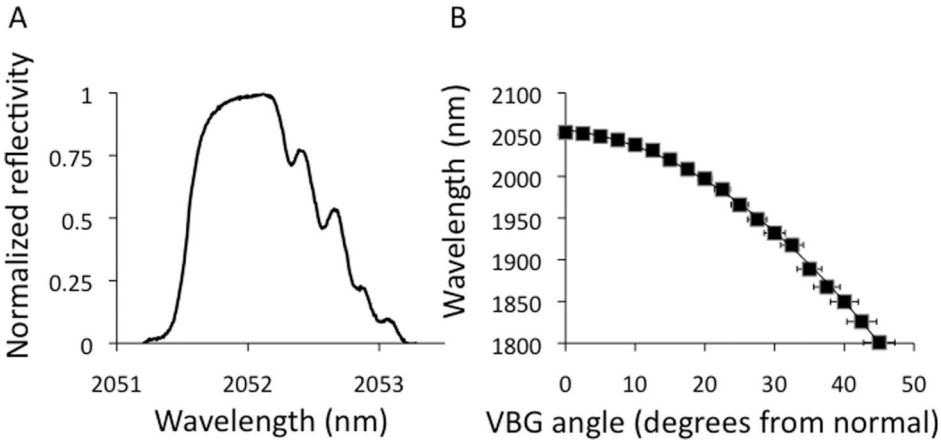

Fig. 4. A, Reflectivity spectrum of the VBG at normal incidence. B, VBG reflectivity as a function of the angle of incidence from normal.

of a higher reflectivity output coupler [24], but this would hurt system performance at wavelengths lower than ~2100 nm. Likewise, the tuning edge can be significantly extended to shorter wavelengths by core pumping the Tm:fiber at 1565 nm and reducing the active fiber length [9]. We chose the best compromise in terms of laser tuning range, performance, and fiber length as described in [19].

Slope efficiency is 30%–35% with respect to total pump power. The relatively low slope efficiency is due to the <90% reflectivity of the diffraction grating, loss from the intracavity beam splitter cube, and loss in the pump combiner because it is not optimized for bidirectional intracavity use. The MO linewidth is <200 pm FWHM across the entire tuning range up to 12 W output power with no sign of ASE or parasitic lasing, as measured by an optical spectrum analyzer with 50 pm resolution (Yokogawa Electric Corporation). An example of output spectrum at one test wavelength is seen in Fig. 5B. Beam quality (inset Fig. 5B) from the MO is excellent, and the mode stripper eliminates unwanted light in the cladding.

The output polarization is linear at all wavelengths with a PER of >20 dB. For seeding the PA, the output power of the MO is limited to ~8.5 W to maximize laser stability. This is sufficient for transmission, with ~80 to 93% efficiency (wavelength dependent), through a free-space isolator and to saturate the PA. It is important to note that the isolator caused thermal lensing, and though the lens was relatively uniform and did not distort the beam, it does affect the alignment between the MO and PA. This thermal lens changes with seed power and seed wavelength; thus, the system alignment has to be adjusted slightly when the seed conditions are changed.

After the isolator, the MO seed beam is aligned and its mode field diameter matched to that of the LMA PA fiber with an overall coupling efficiency of 75%, including reflection losses in the optical path. The highest slope efficiency is achieved at 1967 nm, at ~65% with respect to launched pump power with ~6.3 W of seed coupled into the amplifier fiber

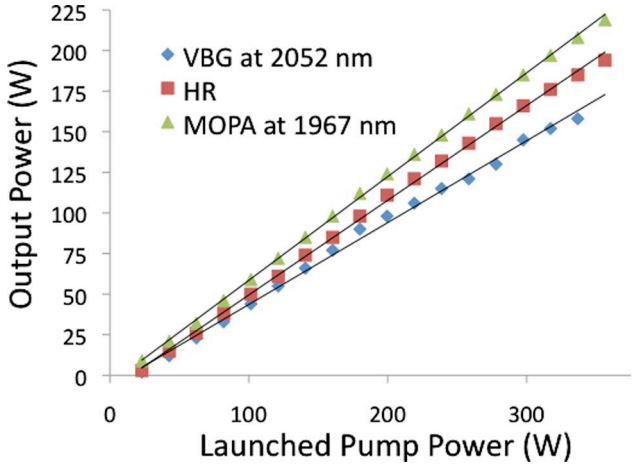

Fig. 6. (Color online) Optimized laser slope efficiency in oscillator and MOPA configurations.

(Fig. 6), well above the quantum defect limit of ~39% for 790 nm pumped thulium corresponding to efficient cross relaxation. The pump absorption cannot be readily characterized due to the bidirectional free-space pumping scheme; however, it is estimated to be ~90 to 95%. There is a slight roll-off in efficiency at higher output powers, because the wavelength of the pump diodes redshift from 793 nm at the highest powers; however, it is not possible to cool the diodes further without causing significant water condensation and this reduction in slope efficiency is deemed insufficient to demand a reoptimization of the amplifier configuration. Maximum output power is 218 W at 1967 nm with ~360 W pump power. More pump power is available; however, the fraction of improperly coupled light is sufficient to cause catastrophic thermal damage to the fiber polymer near the fiber facet. Improved coupling efficiency and higher output powers are possible using high-power fiber-based pump combiners [11]. M^2 is measured to be <1.2, invariant of power. The resolution of this measurement was limited by the large (~80 μm) pixel size of the Spiricon Pyrocam used for beam profiling and the optics available for the measurement.

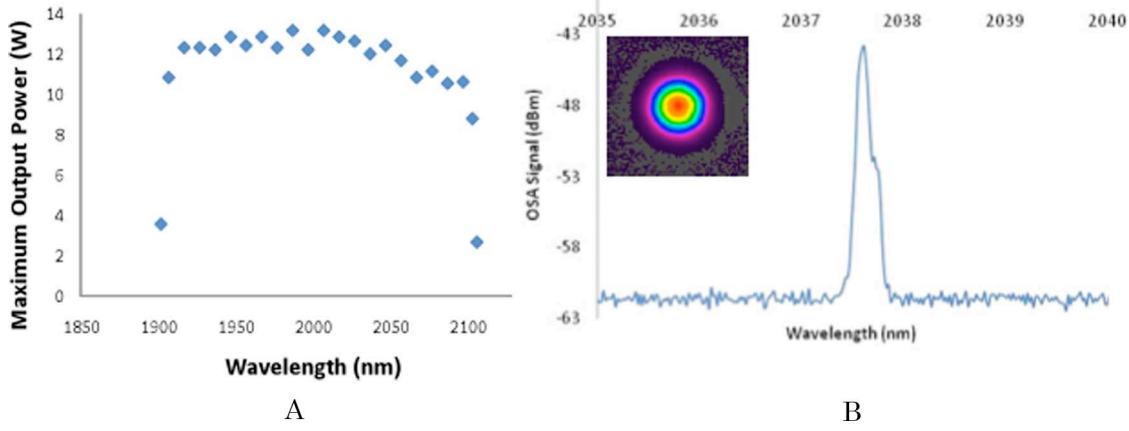

Fig. 5. (Color online) A, MO output power versus wavelength. B, Representative output spectrum and beam image (inset).

Other researchers using similar thulium LMA fiber and high resolved beam diagnostic equipment have demonstrated M^2 as low as 1.05 [23].

For the same ~360 W pump power, >200 W output power is achieved from 1927 nm to 2097 nm (Fig. 7). The short wavelength cutoff in the PA is limited by excessive reabsorption of the seed before sufficient net gain can occur to frustrate parasitic lasing. The long wavelength tuning is primarily determined by the tuning range of the MO. The tuning range is also affected by the isolator, which is less effective away from the design wavelength of 2050 nm, thereby increasing the probability of feedback from the PA to the MO. The active PA fiber length of 5 m was chosen, as it provided the best match to the tuning range of the MO with a bias toward the long wavelength edge. As such, the overall tuning range of the MOPA results from several compromises in the performance of the individual components of the system. The amplified spectrum shows no sign of parasitic lasing or ASE, and the linewidth is 150 to 200 pm FWHM with no distortion relative to the MO.

B. High-Power Oscillator

The performance of the high-power oscillator is shown in Fig. 6, relative to the MOPA system for HR and VBG feedback elements (Fig. 3A). Using the VBG for cavity feedback, the maximum power is 159 W for ~330 W of launched pump with 54% slope efficiency before the onset of lasing near the ASE peak. With the HR providing feedback, the output power at ~330 W of launched pump increases to 185 W and the slope efficiency increases to 60%. As with the MOPA system, there is a slight roll-off in slope efficiency at the highest powers due to the shift of the pump wavelength.

The difference in slope efficiency performance between the VBG system and the HR mirror system is primarily due to the lack of AR coatings, the relatively low 95% reflectivity of the VBG, and the difference between the VBG wavelength and the gain peak of this fiber system. With an improved VBG, there is almost no difference in system efficiency between the VBG and HR system [15,25]. As with the MOPA, the M^2 is <1.2 when the system is configured as a high-power oscillator.

The spectral performance in Fig. 8 shows a very narrow line centered at 2052.5 nm for the VBG stabilized cavity versus several unstable spectral peaks spanning 20–30 nm centered at ~2030 nm. For the HR system, the center wavelength and the number of peaks varied with time and incident pump power, whereas the VBG spectrum stayed locked at 2052 nm regardless of run time or power level. However, as shown in Fig. 4B), the reflectivity band of the VBG is a rather square-shaped ~1.2 nm wide window. The flattop nature of the VBG reflectivity allows laser wavelength to vary within this range. The variation of the VBG laser spectrum with increasing power is shown in Fig. 9. The center wavelength remains within an ~0.3 nm range, while the linewidth 10 dB down from the spectral peak varies from ~0.3 to 1.5 nm. Improved linewidth control is possible with the reduced VBG reflectivity bandwidth. Volume Bragg grating stabilized lasers have been demonstrated with <0.2 nm FWHM linewidths at other wavelengths [13,25–27].

The high-power oscillator is operated in a tunable regime using the VBG reflectivity as a function of the angle of incidence shown in Fig. 4B. Tunability is achieved by rotating the VBG about its axis with a HR mirror to feed back to the laser cavity. The laser was tuned from 1947 nm (~30° incident angle) up to 2052 nm (normal incidence), and the output power relative to wavelength for a fixed pump power of ~120 W is seen in Fig. 7. The maximum output power of 48 W was the maximum achievable before the onset of parasitic lasing. From Fig. 7, it is clear that the MOPA system offers higher power and wider tunability; however, the tunable performance of the VBG system could be improved with several modifications. For example, polishing the sides of the VBG would reduce the amount of light scattered when used at nonnormal incidence, and thereby significantly increase the threshold for parasitic lasing

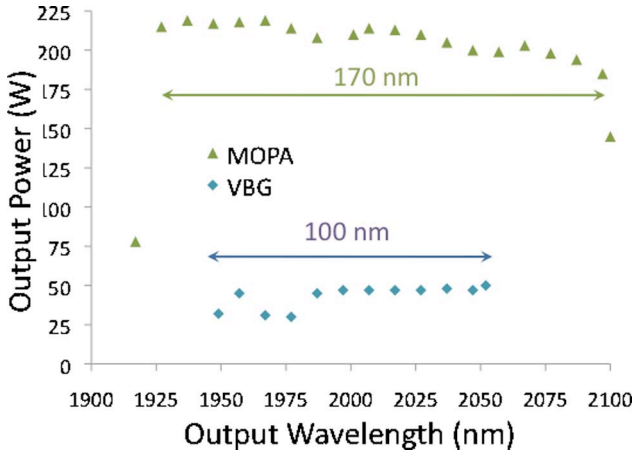

Fig. 7. (Color online) Tm:fiber laser tunability using MOPA and VBG stabilized oscillator configurations.

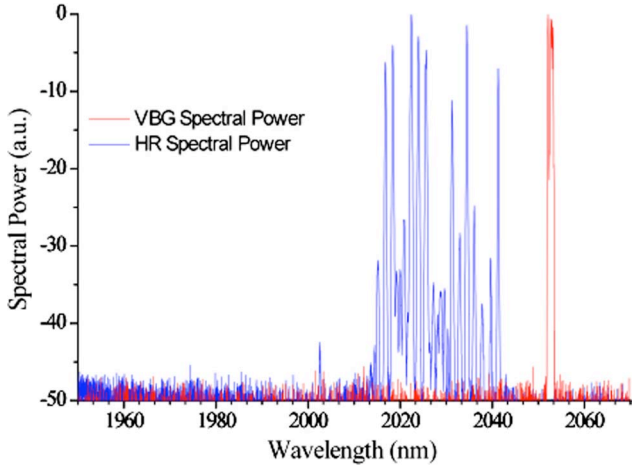

Fig. 8. (Color online) High-power oscillator output spectrum for HR and VBG, respectively.

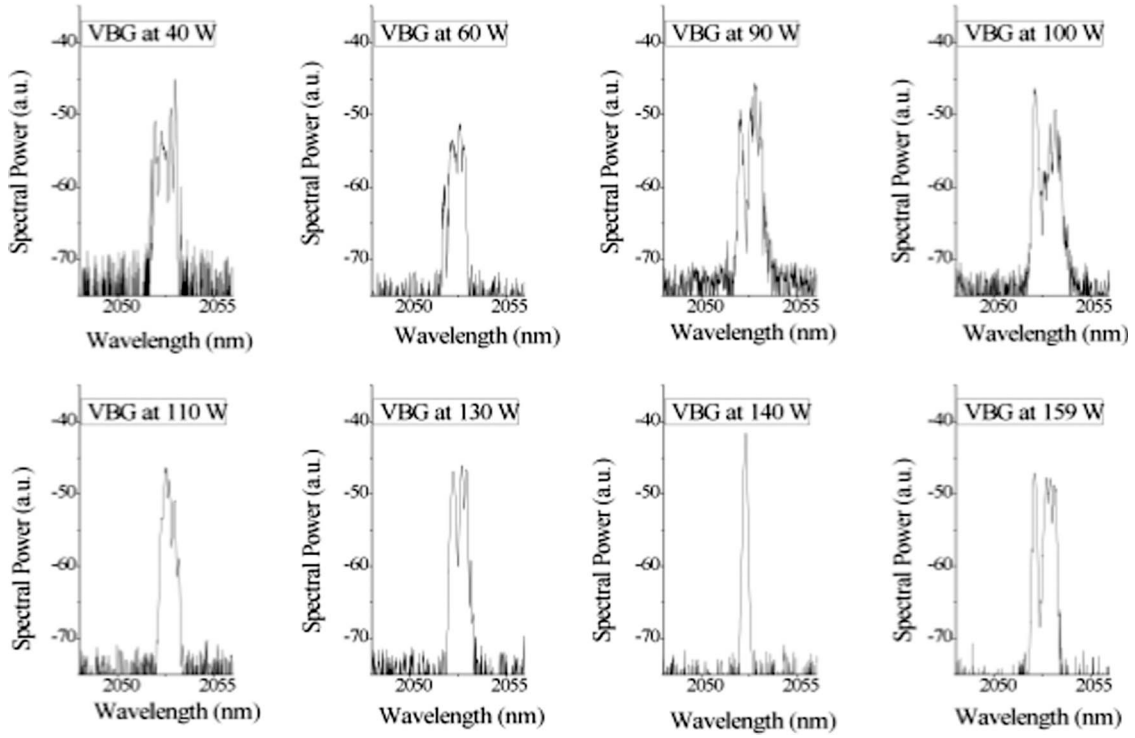

Fig. 9. Volume Bragg grating spectral performance at various output powers.

due to undesirable feedback. The long wavelength tuning edge is set by the Bragg condition at normal incidence, whereas the short wavelength edge is limited by increased losses from Fresnel reflections, decreased reflectivity, and vignetting of the beam by the VBG aperture at a high angle in addition to self-absorption from the three-level nature of thulium lasers.

4. Discussion

Here we have reported the performance of two different tunable high-power Tm:fiber laser configurations. The highest power, widest tunability, and narrowest linewidth are provided using a MOPA architecture in which the relatively low power oscillator is optimized for wide tunability and narrow linewidth, while the high-PA is optimized for maximum power and efficiency. The system described here utilizes a PM single-mode oscillator generating >10 W average power from 1907 to 2098 nm, and an amplifier generating >200 W from 1927 to 2097 nm with <200 pm linewidth.

However, this performance adds complexity and cost, which is enhanced by the immaturity of components in the 2 μm wavelength regime. Therefore, a high-power Tm:fiber oscillator laser architecture is highly desirable. We show that narrow linewidth, broad tunability, high output, and high efficiency can be achieved simultaneously by using a VBG for intracavity feedback. The maximum output power was 159 W, limited by parasitic lasing. The output linewidth was <1.5 nm, and the output was tunable from 1947 to 2053 nm with 30 to 50 W of output power.

Utilizing the same fiber and pump setup in different cavity configurations, the highest slope efficiency of 65% was achieved as an amplifier at 1967 nm. This slope efficiency reduced to 60% when the system was operated as an oscillator with a free-running wavelength around $\sim$2030 nm, which further decreased to 54% with the VBG stabilized oscillator at 2052 nm. Relatively modest improvements to the VBG properties (increasing the reflectivity, adding AR coatings, reducing the reflectivity window, and increasing the clear aperture) enable significant improvements such as increased slope efficiency, higher output power, narrower linewidth, and parasitic lasing suppression. With such improvements in laser performance, the simplicity of a VBG-based tunable high-power Tm:fiber oscillator would be very attractive for novel applications.

The authors would like to acknowledge support and funding from the Joint Technology Office (Multiple Research Initiative contract W91NF-05-1-0517) and the State of Florida.

References

1. T. Giorgio, V. Sudesh, M. C. Richardson, M. Bass, A. Toncelli, and M. Tonelli, "Temperature-dependent spectroscopic properties of Tm3+ in germanate, silica and phosphate glasses: a comparative study," J. Appl. Phys. **103**, 093104 (2008).
2. P. Sprangle, A. Ting, J. Penano, R. Fischer, and B. Hafizi, "Incoherent combining and atmospheric propagation of high-power fiber lasers for directed-energy applications," IEEE J. Quantum Electron. **45**, 138–148 (2009).
3. F. Hanson, P. Poirier, D. Haddock, D. Kichura, and M. Lasher, "Laser propagation at 1.56 μm and 3.60 μm in maritime environments," Appl. Opt. **48**, 4149–4157 (2009).

4. S. Ishii, K. Mizutani, H. Fukuoka, T. Ishikawa, B. Philippe, H. Iwai, T. Aoki, T. Itabe, A. Sato, and K. Asai, "Coherent 2 μm differential absorption and wind lidar with conductively cooled laser and two-axis scanning device," Appl. Opt. **49**, 1809–1817 (2010).
5. G. J. Koch, J. Y. Beyon, B. W. Barnes, M. Petros, J. Yu, F. Amzajerdian, M. J. Kavaya, and U. N. Singh, "High-energy 2 μm Doppler lidar for wind measurements," Opt. Eng. **46**, 116201 (2007).
6. R. J. De Young and N. P. Barnes, "Profiling atmospheric water vapor using a fiber laser LIDAR system," Appl. Opt. **49**, 562–567 (2010).
7. R. C. Stoneman and L. Esterowitz, "Efficient, broadly tunable, laser-pumped Tm:YAG and Tm:YSGG cw lasers," Opt. Lett. **15**, 486–488 (1990).
8. S. D. Jackson, "Cross relaxation and energy transfer upconversion processes relevant to the functioning of 2 μm Tm^{3+}-doped silica fibre lasers," Opt. Commun. **230**, 197–203 (2004).
9. W. A. Clarkson, L. Pearson, Z. Zhang, J. W. Kim, D. Shen, A. J. Boyland, J. K. Sahu, and M. Ibsen, "High power thulium doped fiber lasers," in *Optical Fiber Communication Conference*, OSA Technical Digest (CD) (Optical Society of America, 2009), paper OWT1.
10. G. P. Frith and D. G. Lancaster, "Power scalable and efficient 790 nm pumped Tm-doped fiber lasers," Proc. SPIE **6102**, 610208 (2006).
11. T. Ehrenreich, R. Leveille, I. Majid, K. Tankala, G. Rines, and P. Moulton, "1 kW, all-glass Tm:fiber laser," Proc. SPIE **7580**, xxxvii (2010).
12. T. Erdogan, "Fiber grating spectra," J. Lightwave Technol. **15**, 1277–1294 (1997).
13. J. W. Kim, P. Jelger, J. K. Sahu, F. Laurell, and W. A. Clarkson, "High-power and wavelength-tunable operation of an Er,Yb fiber laser using a volume Bragg grating," Opt. Lett. **33**, 1204–1206 (2008).
14. S. Babin, S. Kablukov, and A. Vlasov, "Tunable fiber Bragg gratings for application in tunable fiber lasers," Laser Phys. **17**, 1323–1326 (2007).
15. T. McComb, V. Sudesh, and M. Richardson, "Volume Bragg grating stabilized spectrally narrow Tm fiber laser," Opt. Lett. **33**, 881–883 (2008).
16. F. Wang, D. Shen, D. Fan, and Q. Lu, "Spectrum narrowing of high power Tm: fiber laser using a volume Bragg grating," Opt. Express **18**, 8937–8941 (2010).
17. A. A. Mehta, R. C. Rumpf, Z. A. Roth, and E. G. Johnson, "Guided mode resonance filter as a spectrally selective feedback element in a double-cladding optical fiber laser," IEEE Photon. Technol. Lett. **19**, 2030–2032 (2007).
18. R. A. Sims, Z. Roth, T. McComb, L. Shah, V. Sudesh, P. Menelaos, E. Johnson, and M. C. Richardson, "Guided mode resonance filters as stable line-narrowing feedback elements for Tm fiber lasers," in *Conference on Lasers and Electro-Optics / International Quantum Electronics Conference*, OSA Technical Digest (CD) (Optical Society of America, 2009), paper CThN2.
19. W. A. Clarkson, N. P. Barnes, P. W. Turner, J. Nilsson, and D. C. Hanna, "High-power cladding-pumped Tm-doped silica fiber laser with wavelength tuning from 1860 to 2090 nm," Opt. Lett. **27**, 1989–1991 (2002).
20. T. S. McComb, L. Shah, R. A. Sims, V. Sudesh, J. Szilagyi, and M. Richardson, "High power, tunable thulium fiber laser system for atmospheric propagation experiments," in *Conference on Lasers and Electro-Optics / International Quantum Electronics Conference*, OSA Technical Digest (CD) (Optical Society of America, 2009), paper CThR5.
21. G. P. Frith, B. Samson, A. Carter, J. Farroni, and K. Tankala, "High efficiency 110 W monolithic FBG tuned 2 μm fiber laser," in *CLEO / Europe and IQEC 2007 Conference Digest* (Optical Society of America, 2007), paper CJ4_5.
22. L. Pearson, J. W. Kim, Z. Zhang, M. Ibsen, J. K. Sahu, and W. A. Clarkson, "High-power linearly-polarized single-frequency thulium-doped fiber master-oscillator power-amplifier," Opt. Express **18**, 1607–1612 (2010).
23. G. D. Goodno, L. D. Book, and J. E. Rothenberg, "Low-phase-noise, single-frequency, single-mode 608 W thulium fiber amplifier," Opt. Lett. **34**, 1204–1206 (2009).
24. Z. S. Sacks, Z. Schiffer, and D. David, "Long wavelength operation of double-clad Tm:silica fiber lasers," Proc. SPIE **6453**, 645320 (2007).
25. F. Wang, D. Shen, D. Fan, and Q. Li, "Widely tunable dual-wavelength operation of a high-power Tm:fiber laser using volume Bragg grating," Opt. Lett. **35**, 2388–2391 (2010).
26. O. M. Efimov, L. B. Glebov, K. C. Glebova, K. C. Richardson, and V. I. Smirnov, "High-efficiency Bragg gratings in photothermorefractive glass," Appl. Opt. **38**, 619–627 (1999).
27. P. Jelger, P. Wang, J. K. Sahu, F. Laurell, and W. A. Clarkson, "High-power linearly-polarized operation of a cladding-pumped Yb fibre laser using a volume Bragg grating for wavelength selection," Opt. Express **16**, 9507–9512 (2008).